Supporting Information

Strong, machinable and insulating chitosan-urea aerogels: towards ambient pressure drying of biopolymer aerogel monoliths

Natalia Guerrero Alburquerque[1,2], Shanyu Zhao[1]*, Nour Adilien[1], Matthias M. Koebel[1], Marco Lattuada[2], Wim J. Malfait[1]*

[1] *Laboratory for Building Energy Materials and Components, Swiss Federal Laboratories for Materials Science and Technology, Empa, Überlandstrasse 129, CH-8600 Dübendorf, Switzerland*

[2] *Department of Chemistry, University of Fribourg, Chemin du Musée 9, CH-1700 Fribourg, Switzerland*

* wim.malfait@empa.ch, +41 58 765 4983; shanyu.zhao@empa.ch, +41 58 765 4244

Figure S1. Thermal conductivity device

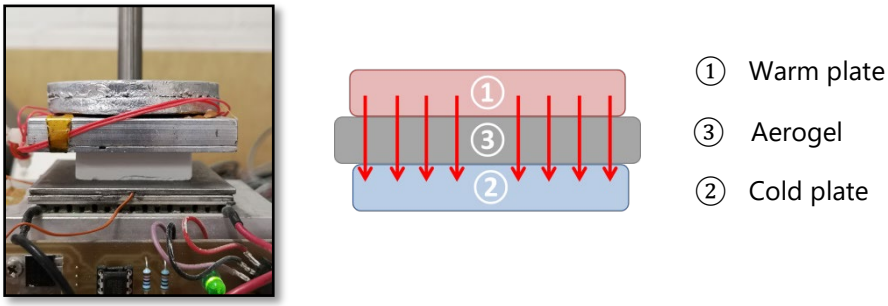

Figure S2. Humidity uptake

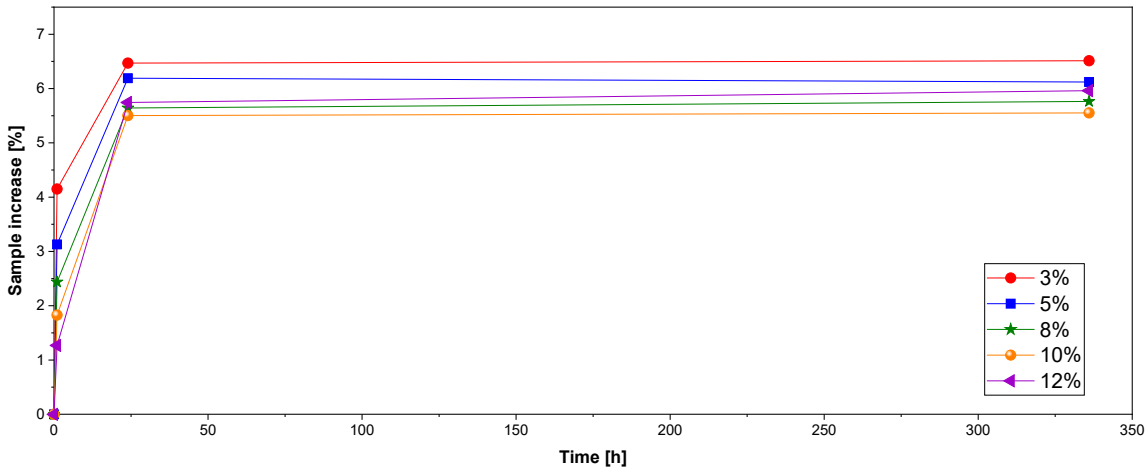

Figure S3. Nitrogen sorption isotherms and BJH pore sizes distributions for all chitosan concentrations

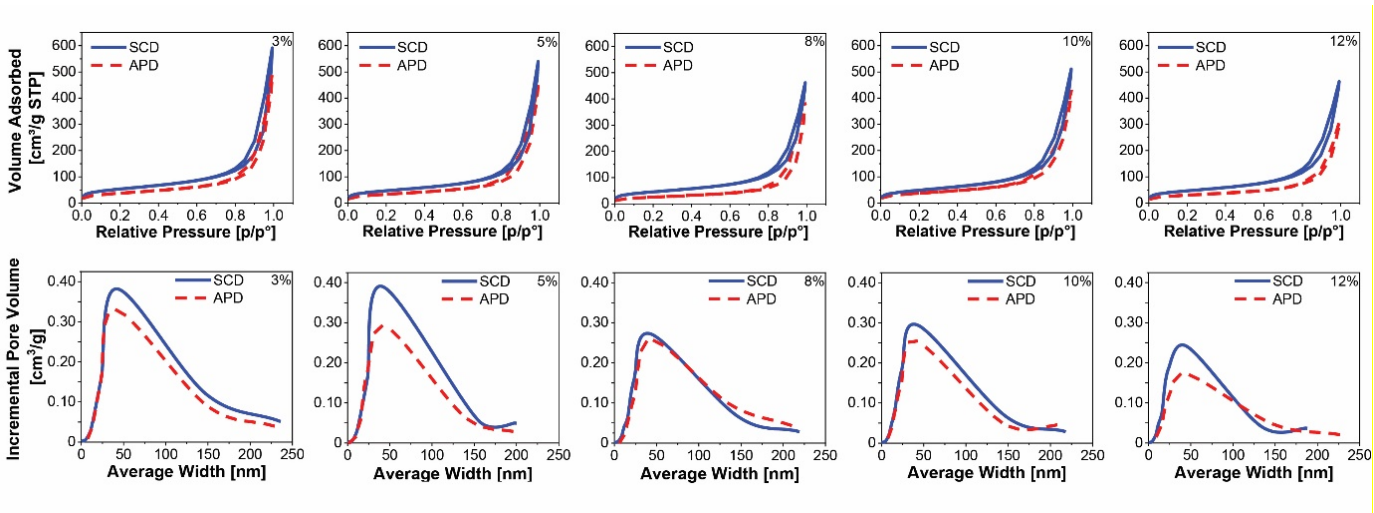

Figure S4. Burning test SCD 10% m/v chitosan aerogel

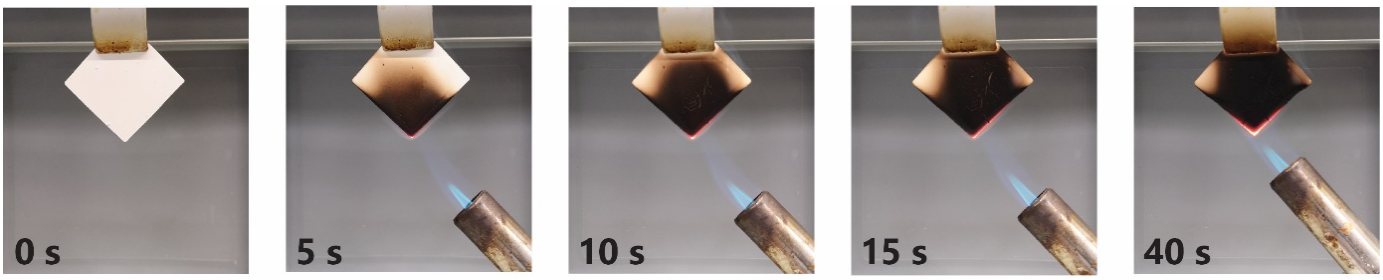

Figure S5. Simulated reaction between 100'000 amino groups and 833'333 urea molecules (equivalent to a urea:d-glucosamine ratio of 6, and a degree of deacetylation of 72%), assuming equal probabilities for the end-capping (ureido) and cross-linking (ureylene) reaction. Because of the large urea excess, probability for cross-linking (a reaction between a ureido group and an amino group) remains low and the final fraction of ureylene cross-linking is limited to 3%.

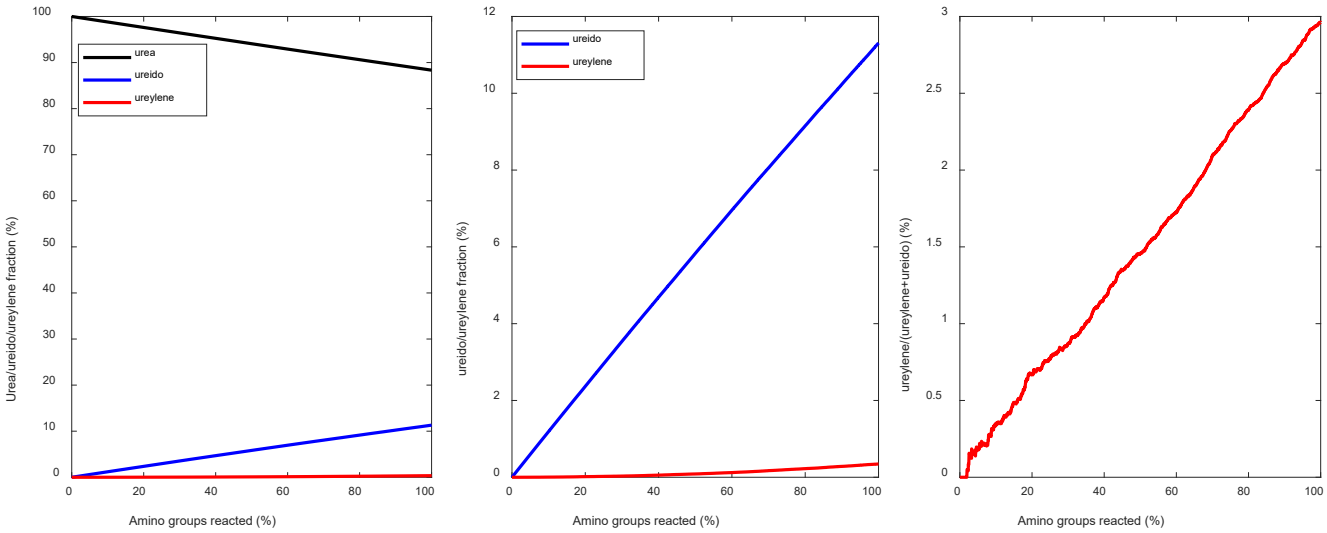

Table S1: Reagent concentrations

	Chitosan [% m/v]	**HCl [M]**	**HCl sol. [mL]**	**Chitosan [g]**	**Urea [g]**	**CTAC [mL]**
SCD Samples	3 %	0.34 M	40	1.2	2.68	0.030
	5 %	0.56 M		2.0	4.47	
	8 %	0.89 M		3.2	7.16	
	10 %	1.12 M		4	9	
	12 %	1.34 M		4.8	10.73	
APD Samples	3 %	0.34 M	120	3.6	8.04	0.090
	5 %	0.56 M		6	13.41	
	8 %	0.89 M		9.6	21.48	
	10 %	1.12 M		12	27	
	12 %	1.34 M		14.4	32.19	

Table S2: Influence of chitosan:urea ratio on gelation and properties

10% (m/v) of chitosan in HCl aq. (1.12M)		
Ratio [Chitosan:Urea]	**Gelation after 24h at 80°C**	**λ [mW /(m·K)]**
1:0,5	No	-
1:1	No	-
1:2	No	-
1:3	No	-
1:4	Yes	28.1 ± 0.2
1:6	Yes	23.1 ± 0.3

Table S3: Temperature and time reaction influence

5% (m/v) of chitosan in HCl aq. (0.56 M) Chitosan:Urea = 1:6 Reaction temperature and time = 80 °C, 24h			
T [°C]	**Time [h]**	**Gelation**	**λ [mW /(m·K)]**
70	24	No	-
70	48	No	-
80	5	Yes	22.6 ± 0.1
80	12	Yes	22.8 ± 0.2
80	24	Yes	25.5 ± 0.2
80	48	Yes	23.5 ± 0.2
90	5	Yes	23.6 ± 0.1
90	12	Yes	24.4 ± 0.3
90	24	Yes	22.1 ± 0.1
90	48	Yes	25.4 ± 0.3

Table S4: HCl concentration influence

Chitosan:Urea = 1:6 Reaction temperature and time = 80 °C, 24h				
Protonation	**Chitosan HW conc.**	**HCl conc.**	**Gelation**	**λ [mW /(m·K)]**
76.5 %	3 %	0.14 M	Yes	37.9 ± 0.2
90 %	3 %	0.17 M	Yes	36.1 ± 0.2
90 %	10 %	0.56 M	Yes	40.1 ± 0.5
180 %	10 %	1.12 M	Reference: Yes	22.4 ± 0.3

Table S5: Chitosan molecular weight influence

Low molecular weight (LW), 50'000–190'000 g/mol; η <200 mPa·s (1% acetic acid, 20 °C) Medium molecular weight (MW), 190'000-310'000 g/mol; η=200-400 mPa·s (1% acetic acid, 20 °C) High molecular weight (HW) = 310'000 – 375'000 g/mol; η = >400 mPa·s (1% acetic acid, 20 °C) Chitosan:Urea = 1:6, Reaction temperature and time = 80 °C, 24h	
Molecular weight	**Gelation**
LW	No
MW	No
HW	Yes

Table S6: Solubility of chitosan HW in different acids

Dissolving temperature = 70 °C				
Chitosan % [m/v]	**Acid**	**Acid conc.**	**Dissolution time**	**Observation**
10 %	Acetic acid	99%	2 h	No dissolution
5 %	Acetic acid	99%	6 h	No dissolution
5 %	Acetic acid in water	50 %	4 h	Very viscous gel, not usable
10 %	Trichloroacetic acid	99%	6 h	No dissolution
10 %	Trichloroacetic acid	50%	6 h	No dissolution
10 %	Trifluoroacetic acid	95%	10 min	Dissolved but after aging got carbonized
10 %	Trifluoroacetic acid in water	50 %	2h 30 min	Dissolved but after aging got carbonized

Table S7: Peak positions, assignment and intensities of Solid-state CP-MAS ^{13}C NMR

$\delta^{13}C$ [ppm]	Assignment #	Central band	ssb	Intensity [a] [%]	Intensity (total) [a,b] [%]
240.8	9*		Ureido	1	
214.4	7*		Acetyl C=O	5	
200.9	9*		Ureido	11	
174.5	7	Acetyl C=O		11	22
161.2	9	Ureido		51	77
144.7	1*		Chitosan C1	3	
134.9	7*		Acetyl C=O	6	
123.4	4*		Chitosan C4	4	
121.6	9*		Ureido	13	
115.2	3/5*		Chitosan C3+C5	10	
104.6	1	Chitosan C1		97	100
96.5	2*		Chitosan C2	13	
83.3	4	Chitosan C4		92	108
75.2	3/5	Chitosan C3+C5		206	225
61.2	6	Chitosan C6		87	91
56.1	2	Chitosan C2		103	120
44.3	4*		Chitosan C4	12	
35.6	3/5*		Chitosan C3+C5	10	
23.9	8	Acetyl CH_3		23	23
21.1	6*		Chitosan C6	4	
16.4	2*		Chitosan C2	4	

ssb: spinning sideband

[a] Integrated intensity, as a percentage of the chitosan C1 total intensity

[b] Sum of central band and spinning sidebands

Table S8: FTIR peak positions and assignments

Urea	Assignment	Chitosan	Aerogel: Chitosan-Urea	Assignment
Wavenumber [cm^{-1}]		Wavenumber [cm^{-1}]	Wavenumber [cm^{-1}]	
1000	C-N stretching	992		C-O stretching
1046	NH_2 rocking	1030	1030	
		1065	1067	
			1111	C-O-C stretching
1152	NH_2 rocking	1151	1156	
		1198	1203	OH bending
		1258	1263	
		1307	1309	C-N stretching Amide III
		1376	1376	CH bending CH_3 deformation
1457	C-N stretching	1422		CH_2 bending
			1560	N-H bending Amide II
1590	NH_2 scissoring	1590		NH_2 scissoring
1678	C=O stretching	1650	1650	C=O stretching Amide I
		2871	2877	C-H stretching
		2919	2941	
			3118	N-H stretching
3255	N-H stretching	3290	3282	
3329		3358	3361	O3-H stretching
3429			3453	O6-H stretching

Table S 9. Theoretical relationships between surface area and particle size

Single particle			**1 g chitosan @1.59 g/cm3**		
diameter_p [m]	volume_1p [m^3]	area_1p [m^2]	volume_1g [m^3]	#particles_1g	surface area_1g [m^2/g]
0.00000009	3.815E-22	2.54462E-14	6.28931E-07	1.64857E+15	41.9
0.00000005	6.5415E-23	7.85375E-15	6.28931E-07	9.61447E+15	75.5
0.00000002	4.18656E-24	1.2566E-15	6.28931E-07	1.50226E+17	188.8
	=(4/3)*π*(diameter_p/2)^3 $V = 4/3\pi r^3$	=π*(diameter_p)^2 $A = 4\pi r^2$	=10^-6/1.59	=volume_1g/volume_1p	=#particles_1g*area_1p

Table S10. Chitosan-urea aerogel properties

	Chit. [%]	ρ [g/cm³]			Porosity [%]		V_{pore} [cm³/g]			$V_{pore\ BJH\ Ads.}$ [cm³/g]		$V_{pore\ BJH\ Des.}$ [cm³/g]		S_{BET} [m²/g]			C - value		D_{pore} [nm]			$D_{pore\ BJH\ Ads.}$ [nm]		$D_{pore\ BJH\ Des.}$ [nm]		λ [mW/(m·K)]	
		Av.	SD	N	Av.	SD	Av.	SD	N	Av.	SD	Av.	SD	Av.	SD	N	Av.	SD	Av.	SD	N	Av.	SD	Av.	SD	Av.	SD
SCD	3	0.094	0.018	5	91.8	1.7	9.9	1.9	3	0.8	0.1	0.8	0.1	165	20	3	144	9	245	68	3	22.5	2.1	21.3	1.8	24.1	0.9
	5	0.121	0.024	3	90.0	2.0	8.1	2.0	3	0.8	0.1	0.8	0.1	172	17	3	173	40	190	51	3	21.7	0.9	20.7	0.7	25.7	0.2
	8	0.145	0.021	4	88.0	1.7	6.4	1.0	4	0.7	0.0	0.7	0.0	159	3	4	140	13	160	22	4	20.8	0.9	20.1	0.8	27.8	1.9
	10	0.144	0.013	10	87.5	1.1	6.0	0.6	5	0.7	0.1	0.7	0.1	160	8	5	154	30	152	21	5	20.2	1.4	19.1	1.4	27.9	2.9
	12	0.152	0.011	4	87.3	0.9	5.9	0.5	3	0.7	0.0	0.7	0.0	167	7	3	124	4	141	10	3	19.4	0.5	18.4	0.4	26.2	3.8
APD dried at RT	3	0.305	0.138	4	79.4	9.5	4.9	2.2	3	0.9	0.1	0.9	0.1	150	12	3	119	12	131	51	3	25.3	0.8	23.0	0.5	37.5	0.0
	5	0.361	0.142	4	66.3	11.1	2.8	1.2	3	0.7	0.0	0.7	0.0	127	14	3	117	12	87	26	3	25.1	1.1	21.9	0.4	62.5	19.8
	8	0.423	0.138	3	65.1	11.3	2.7	1.2	3	0.5	0.1	0.5	0.1	83	16	3	147	31	149	95	3	26.8	2.2	23.7	0.2	68.1	25.1
	10	0.278	0.026	4	75.9	0.5	3.4	0.1	3	0.7	0.0	0.7	0.0	134	0	3	125	8	102	3	3	22.3	0.6	20.5	0.9	41.6	3.1
	12	0.225	0.005	3	81.4	0.4	4.4	0.1	3	0.5	0.1	0.5	0.1	106	20	3	156	51	173	35	3	20.3	1.2	20.0	0.9	36.3	0.3
APD dried at 65 °C	5	0.292	0.008	2	74.4	1.2	2.6	0.1	2	1.0	0.0	1.0	0.0	210	0	2	118	0	49	3	2	21.2	0.3	20.0	0.1	44.5	1.0
	8	0.304	0.000	2	76.3	0.0	2.9	0.0	2	0.4	0.4	0.8	0.0	174	2	2	135	4	65	0	2	21.2	0.7	19.9	0.8	55.6	4.0
	10	0.180	0.007	2	85.0	0.4	4.9	0.2	2	0.9	0.0	0.9	0.0	228	7	2	115	6	108	0	2	21.3	0.7	19.4	0.4	37.0	0.8
	12	0.167	0.006	2	86.2	0.4	5.3	0.2	2	1.0	0.0	1.0	0.0	227	5	2	139	16	94	6	2	19.2	0.1	18.0	0.0	30.9	1.0

Table S11

See separate Excel file.

Data sources: [1,2,11–17,3–10]

(1) Zhou, J.; Hsieh, Y.-L. Nanocellulose Aerogel-Based Porous Coaxial Fibers for Thermal Insulation. *Nano Energy* **2020**, *68* (November 2019), 104305. https://doi.org/10.1016/j.nanoen.2019.104305.

(2) Wang, D.; Peng, H.; Yu, B.; Zhou, K.; Pan, H.; Zhang, L.; Li, M.; Liu, M.; Tian, A.; Fu, S. Biomimetic Structural Cellulose Nanofiber Aerogels with Exceptional Mechanical, Flame-Retardant and Thermal-Insulating Properties. *Chem. Eng. J.* **2020**, *389* (December 2019), 124449. https://doi.org/10.1016/j.cej.2020.124449.

(3) Jin, H.; Zhou, X.; Xu, T.; Dai, C.; Gu, Y.; Yun, S.; Hu, T.; Guan, G.; Chen, J. Ultralight and Hydrophobic Palygorskite-Based Aerogels with Prominent Thermal Insulation and Flame Retardancy. *ACS Appl. Mater. Interfaces* **2020**, *12* (10), 11815–11824. https://doi.org/10.1021/acsami.9b20923.

(4) Zhu, J.; Hu, J.; Jiang, C.; Liu, S.; Li, Y. Ultralight, Hydrophobic, Monolithic Konjac Glucomannan-Silica Composite Aerogel with Thermal Insulation and Mechanical Properties. *Carbohydr. Polym.* **2019**, *207*, 246–255. https://doi.org/10.1016/j.carbpol.2018.11.073.

(5) Zhou, S.; Apostolopoulou-Kalkavoura, V.; Tavares da Costa, M. V.; Bergström, L.; Strømme, M.; Xu, C. Elastic Aerogels of Cellulose Nanofibers@Metal–Organic Frameworks for Thermal Insulation and Fire Retardancy. *Nano-Micro Lett.* **2019**, *12* (1), 9. https://doi.org/10.1007/s40820-019-0343-4.

(6) Zhang, S.; Huang, X.; Feng, J.; Qi, F.; E, D.; Jiang, Y.; Li, L.; Xiong, S.; Feng, J. Thermal Conductivities of Cellulose Diacetate Based Aerogels. *Cellulose* **2020**, *0123456789*. https://doi.org/10.1007/s10570-020-03084-y.

(7) Gupta, P.; Verma, C.; Maji, P. K. Flame Retardant and Thermally Insulating Clay Based Aerogel Facilitated by Cellulose Nanofibers. *J. Supercrit. Fluids* **2019**, *152*, 104537. https://doi.org/10.1016/j.supflu.2019.05.005.

(8) Song, J.; Chen, C.; Yang, Z.; Kuang, Y.; Li, T.; Li, Y.; Huang, H.; Kierzewski, I.; Liu, B.; He, S.; et al. Highly Compressible, Anisotropic Aerogel with Aligned Cellulose Nanofibers. *ACS Nano* **2018**, *12* (1), 140–147. https://doi.org/10.1021/acsnano.7b04246.

(9) Fricke, M.; Weinrich, D.; Loelsberg, W.; Subrahmanyam, Ra.; Smirnova, I.; Gurikov, P. PROCESS FOR PRODUCING POROUS ALGINATE - BASED AEROGELS. US 2018 / 0258249 A1, 2018.

(10) Nešić, A.; Gordić, M.; Davidović, S.; Radovanović, Ž.; Nedeljković, J.; Smirnova, I.; Gurikov, P. Pectin-Based Nanocomposite Aerogels for Potential Insulated Food Packaging Application. *Carbohydr. Polym.* **2018**, *195*, 128–135. https://doi.org/10.1016/j.carbpol.2018.04.076.

(11) Jiménez-Saelices, C.; Seantier, B.; Grohens, Y.; Capron, I. Thermal Superinsulating Materials Made from Nanofibrillated Cellulose-Stabilized Pickering Emulsions. *ACS Appl. Mater. Interfaces* **2018**, *10* (18), 16193–16202. https://doi.org/10.1021/acsami.8b02418.

(12) Gupta, P.; Singh, B.; Agrawal, A. K.; Maji, P. K. Low Density and High Strength Nanofibrillated Cellulose Aerogel for Thermal Insulation Application. *Mater. Des.* **2018**, *158*, 224–236. https://doi.org/10.1016/j.matdes.2018.08.031.

(13) Groult, S.; Budtova, T. Thermal Conductivity/Structure Correlations in Thermal Super-Insulating Pectin Aerogels. *Carbohydr. Polym.* **2018**, *196*, 73–81. https://doi.org/10.1016/j.carbpol.2018.05.026.

(14) Ahmad, F.; Ulker, Z.; Erkey, C. A Novel Composite of Alginate Aerogel with PET Nonwoven with Enhanced Thermal Resistance. *J. Non. Cryst. Solids* **2018**, *491*, 7–13. https://doi.org/10.1016/j.jnoncrysol.2018.03.023.

(15) Plappert, S. F.; Nedelec, J. M.; Rennhofer, H.; Lichtenegger, H. C.; Liebner, F. W. Strain Hardening and Pore Size Harmonization by Uniaxial Densification: A Facile Approach toward Superinsulating Aerogels from Nematic Nanofibrillated 2,3-Dicarboxyl Cellulose. *Chem. Mater.* **2017**, *29* (16), 6630–6641. https://doi.org/10.1021/acs.chemmater.7b00787.

(16) Fan, B.; Chen, S.; Yao, Q.; Sun, Q.; Jin, C. Fabrication of Cellulose Nanofiber/AlOOH Aerogel for Flame Retardant and Thermal Insulation. *Materials (Basel).* **2017**, *10* (3), 311. https://doi.org/10.3390/ma10030311.

(17) Takeshita, S.; Yoda, S. Chitosan Aerogels: Transparent, Flexible Thermal Insulators. *Chem. Mater.* **2015**, *27* (22), 7569–7572. https://doi.org/10.1021/acs.chemmater.5b03610.